International Journal of Thermophysics, Vol. 27, No. 4, July 2006 (© 2006)
DOI: 10.1007/s10765-006-0079-5

Speed-of-Sound Measurements in *n*-Nonane at Temperatures between 293.15 and 393.15 K and at Pressures up to 100 MPa[1]

S. Lago,[2,3] P. A. Giuliano Albo,[2] and D. Madonna Ripa[2]

Speed-of-sound measurements in liquid phase *n*-nonane (C_9H_{20}) are reported along six isotherms between 293.15 and 393.15 K and at pressures up to 100 MPa. The experimental technique is based on a double reflector pulse-echo method. The acoustic path lengths were obtained by comparison with measurements carried out at atmospheric pressure and ambient temperature in pure water. The values of the speed of sound are characterized by an overall estimated uncertainty of less than 0.2 %. These results were compared with literature values and with predictions of a dedicated equation of state.

KEY WORDS: pulse-echo technique; *n*-nonane; speed of sound.

1. INTRODUCTION

Speed-of-sound measurements in fluids have recently been extensively used to determine the thermodynamic properties of fluids, including the development of equations of state (EOS). This has come about as a result of advances in both experimental methods and associated theoretical models. Moreover, because of the high accuracy which can be achieved in the measurement of the speed of sound, it is possible to calculate other thermodynamic properties of interest by an indirect methodology maintaining an accuracy comparable with direct methods.

[1] Paper presented at the Seventeenth European Conference on Thermophysical Properties, September 5–8, 2005, Bratislava, Slovak Republic.

[2] Istituto Nazionale di Ricerca Metrologica, Strada delle Cacce 91, 10135 Torino, Italy.
[3] To whom correspondence should be addressed. E-mail: lago@inrim.it

Nonane is a reference fluid in viscosity measurements, and recently it has been used in the calibration of instruments employed in density measurements in liquids [1].

As a part of an ongoing research program to measure the physical properties of *n*-alkanes, we performed accurate measurements of the speed of sound of *n*-nonane along six isotherms for temperatures between 293.15 and 393.15 K and at pressures up to 100 MPa. The overall estimated uncertainty of the experimental data is less than 0.2%. The results were compared with literature values [2, 3] and with the predictions of a dedicated equation of state [4]. Comparisons show deviations within 1%. We expect that these results will be useful in the formulation of a new global equation of state for *n*-nonane and in the development of improved thermodynamic models for hydrocarbons systems.

2. EXPERIMENTAL APPARATUS

The speed of sound was measured using the ultrasonic cell and associated apparatus described in detail in a previous paper [5]. The design of this apparatus is based on the double reflector pulse-echo technique [6, 7] and has been chosen because of its good combination of design simplicity and high resolution and accuracy. The double pulse method is based on direct measurement of the delay between echoes coming from two different reflectors.

The principle of the double pulse-echo technique can be described by means of a time–space diagram as shown in Fig. 1. Two co-axial acoustic beams, generated at the origin of the axis system, propagate in opposite directions towards the two steel reflectors with the same speed u. Since the reflectors are placed at different distances from the origin, the acoustic signals return to the source at different times.

A simple geometric consideration of the diagram can be used to obtain the expression for the speed of sound u,

$$u = \frac{2(L_2 - L_1)}{\tau_2 - \tau_1} = \frac{2\Delta L}{\tau}. \tag{1}$$

The static pressure generator consists of three elements: the pressure vessel that contains the measuring cell, the monitoring system consisting of a set of two pressure transducers, and the pressure control device composed of a pressure amplifier and the sample reservoir. The pressure was measured by means of two Sensotec transducers with full-scale ranges of 10 and 206 MPa. The pressure monitoring system switches from one transducer to the other, depending on the pressure, in order to improve the resolution and to reduce the measurement uncertainty.

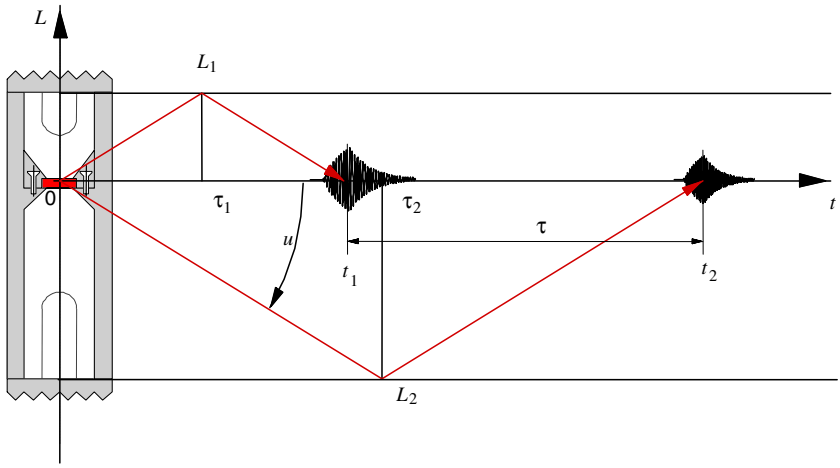

Fig. 1. Schematic of the pulse-echo technique; representation of the time–space diagram.

The ultrasonic cell and pressure vessel were placed in a thermostatic liquid bath. The long-term temperature stability within the bath is about ±1 mK over the whole working range. The temperature value to be associated with each speed of sound measurement was determined (with an uncertainty of ±0.01 K) as the average of the readings of two standard calibrated platinum resistance thermometers (PRTs) attached to the top and bottom parts of the pressure vessel.

2.1. Purity of the Sample

A pure sample of C_9H_{20} (*n*-Nonane) was supplied by the firm Acros Organic. The declared specific mole fraction purity of this sample was better than 99.6 mol%. The major impurities are listed in Table I; no further analysis or purification was attempted. However, the level of impurities present in the sample of *n*-nonane has negligible affect on the speed-of-sound measurements.

Table I. Impurities in the Sample of *n*-Nonane (> 99.6 mol%)

Impurities	Dichlorom-ethane	*n*-Octane	*n*-Nonane isomer	*n*-Decane isomer	Cycloal-canes	Others
(mol%)	not identified	< 0.01	< 0.01	0.32	< 0.01	< 0.01

2.2. Temporal Delay Determination

According to Eq. (1), the experimental technique is based on a high accuracy determination of the difference $(\tau_2 - \tau_1)$ between two fly times. A digital oscilloscope records the two echoes from reflectors with a sampling rate of 4 GS/s. Calculating the correlation function of the two echo signals $P_1(t_i)$ and $P_2(t_j)$ by

$$C(\tau) = \int_{-\infty}^{+\infty} P_1(t) P_2(t+\tau)\, dt = F^{-1}[F[P_1(t)]\, F[P_2(t)]], \tag{2}$$

and choosing a value of the delay time τ which τ maximizes the correlation function $C(\tau)$, it is possible to have a very good estimate of the temporal delay between echoes. A detailed explanation of this method and its signal-to-noise ratio is discussed in [5].

The delay time τ must be increased by a quantity δ_τ, which takes into account diffraction effects due to the finite dimensions of the piezoelectric source according to the following equations:

$$\delta\tau = \frac{\varphi(2L_2) - \varphi(2L_1)}{\omega_0} \tag{3}$$

$$\varphi(L) = \mathrm{Arg}\left(1 - \frac{4}{\pi}\int_0^{\pi/2} \exp\left[-i\left(\frac{2\omega_0 b^2}{uL}\right)\cos^2(\theta)\right]\sin^2(\theta)\, d\theta\right), \tag{4}$$

where ω_0 is the angular frequency of the carrier beam, L_1 and L_2 are the distances that separate the source from each reflector, and b is the radius of the source. The integral in Eq. (4) cannot be evaluated in a closed form; however, if the following condition is assumed,

$$\frac{L_i}{b} > \sqrt[3]{kb}, \quad \text{with } i = 1,\ 2 \tag{5}$$

where $k = 2\pi/\lambda$ is the propagation constant and λ is the ultrasonic wavelength, it is possible to substitute for the expression, Eq. (4), by the approximation,

$$\varphi(\zeta) = \left(1 - \frac{\zeta^2}{2k^2b^2}\right)[J_0(\zeta) + iJ_1(\zeta)]\exp(-i\zeta) - \frac{\zeta^2}{k^2b^2}\left[iJ_1\frac{(\zeta)}{\zeta}\right]\exp(-i\zeta), \tag{6}$$

in which the variables L and ζ are related by the following expression,

$$\frac{L\lambda}{b^2} = \frac{2\pi}{\zeta}\left(1 - \frac{\zeta^2}{k^2b^2}\right). \tag{7}$$

The accuracy and limitations of this method are comprehensively described in [8] where it is possible to find all details about the derivation of Eq. (6) from Eq. (4). The diffraction correction for our experimental apparatus amounted to less than 0.008% of the measured transit time difference.

2.3. Acoustic Path Length Measurement

As shown in Eq. (1), in order to obtain the speed of sound, it is necessary to know the difference of the acoustic path lengths. This determination can be carried out by means of a reference liquid at a fixed thermodynamic state (T_0, p_0) using the equation,

$$\Delta L(T_0, p_0) = u_{\text{calibr}}\Delta\tau_{\text{calibr}}, \tag{8}$$

where u_{calibr} is the known speed of sound of the reference fluid and $\Delta\tau_{\text{calibr}}$ is the measured delay time between echoes in the same fluid at T_0 and p_0.

The difference of path lengths ΔL can be calculated at a different state (T, p) as

$$\Delta L(T, p) = \Delta L\left(T_{0,}p_0\right)[1 + \alpha(T - T_0) - \beta(p - p_0)], \tag{9}$$

where α and β are, respectively, the linear thermal expansion coefficient and the compressibility coefficient of stainless steel 303 [9]. To apply the corrections for diffraction effects, the absolute lengths, L_1 and L_2, are needed, due to the nonlinear nature of Eq. (6).

The procedure described in [10] for single reflector pulse-echo and delay-line techniques was applied to our double reflector apparatus. This is based on the numerical reconstruction of the transfer function $H(f)$ of the piezoelectric transducer around the working frequency f_0.

According to the scheme of our experiment, the piezoelectric transducer operates first as a resonant ultrasonic source and then as a narrow-band receiver. If $P_0(t)$ is the electric pulse applied to the piezoelectric

transducer (and recorded by the oscilloscope), the shape of the acoustic pulse in the liquid is given by

$$P_{\text{acu}}(t) = F^{-1}[H(f)\, F[P_0(t)]], \tag{10}$$

where F indicates the Fourier operator. Since the transducer operates at the resonance to maximize the signal amplitude, $H(f)$ introduces a delay between $P_{\text{acu}}(t)$ and $P_0(t)$. The same transfer function is involved when the acoustic echo $P_{\text{echo}}(t)$ is converted to an electric signal $P_{\text{el\_echo}}(t)$ and recorded by the oscilloscope;

$$P_{\text{echo}}(t) = F^{-1}\left[\frac{F[P_{\text{el\_echo}}(t)]}{H^*(f)}\right]. \tag{11}$$

To work out the acoustic delay time from the experimental data $P_0(t)$ and $P_{\text{el\_echo}}(t)$, the form of $H(f)$ is needed; we suppose it can be represented by a sum of a certain number of Lorentzian functions $H(f|f_i, Q_i)$, parameterized by the peak frequency f_i and quality factor Q_i. Since the absolute values of L_1 and L_2 are needed only to calculate a correction, it is possible to simplify the mathematical model by assuming

$$F[P_{\text{echo}}] = e^{i2\pi\frac{f}{\tau}} F[P_{\text{acu}}], \tag{12}$$

that is, we consider the acoustic propagation in the ultrasonic cell as a simple translation. The following relation can be derived from Eqs. (10–12):

$$|H(f)|^2 = \frac{|F[P_{\text{el\_echo}}]|}{|F[P_0]|}, \tag{13}$$

so the parameter set $\{f_i, Q_i\}$ can be obtained from experimental data ($P_{\text{el\_echo}}(t)$ and $P_0(t)$) using a nonlinear curve fitting algorithm. Note that Eq. (13) only allows the determination of the modulus $|H(f)|$ (a residual phase-shift error can be present).

By means of the reconstructed transfer function $H(f)$, it is possible to correlate the electrical pulse signal $P_0(t)$ with the two echoes $P_i(t)$ (see Eq. (2)), obtaining the transit times for each of the two echoes and then L_1 and L_2 from the speed of sound of the calibration fluid. The accuracy of this procedure is sufficient for a diffraction effect correction.

3. RESULTS

3.1. Results and Comparisons

The measurements were regularly distributed along six isotherms, starting at the highest pressure (100 MPa) and proceeding downward to atmospheric pressure in increments of 10 MPa. The experimental grid in the $T-p$ space and the associated values of speed of sound have been corrected, without introducing a further relevant uncertainty component, in order to obtain a 11×6 regular matrix of points using a fourth order polynomial fit. The experimental values are listed in Table II and presented in Fig. 2 as a function of temperature and pressure.

Moreover, we have compared our results with the predictions of Lemmon and Span [4]. The estimated uncertainty of this formulation is about 1% over the $T-p$ region of interest for our measurements. As shown in Fig. 3, our results show deviations from [4] within 1% for all the temper-

Table II. Experimental Speeds of Sound of *n*-Nonane

P (MPa)	U ($m \cdot s^{-1}$)	P (MPa)	U ($m \cdot s^{-1}$)	P (MPa)	U ($m \cdot s^{-1}$)	P (MPa)	U ($m \cdot s^{-1}$)	P (MPa)	U ($m \cdot s^{-1}$)
				$T = 293.15$ K					
0.1	1226.379	10	1288.02	20	1344.821	30	1396.854	40	1445.084
50	1490.057	60	1532.464	70	1572.512	80	1610.591	90	1646.928
								100	1681.563
				$T = 313.15$ K					
0.1	1146.226	10	1212.824	20	1274.241	30	1329.834	40	1380.943
50	1428.288	60	1472.742	70	1514.719	80	1554.351	90	1592.049
								100	1628.026
				$T = 333.15$ K					
0.1	1068.198	10	1140.94	20	1206.915	30	1266.203	40	1320.126
50	1369.835	60	1416.313	70	1460.059	80	1501.308	90	1540.349
								100	1577.369
				$T = 353.15$ K					
0.1	992.6189	10	1072.568	20	1142.609	30	1205.597	40	1262.461
50	1314.591	60	1363.169	70	1408.501	80	1451.316	90	1491.697
								100	1529.841
				$T = 373.15$ K					
0.1	922.1599	10	1004.987	20	1081.282	30	1148.091	40	1207.979
50	1262.528	60	1313.133	70	1360.053	80	1404.349	90	1446.071
								100	1485.463
				$T = 393.15$ K					
0.1	867.4314	10	946.865	20	1022.924	30	1093.674	40	1156.595
50	1213.59	60	1266.136	70	1314.71	80	1360.387	90	1403.307
								100	1443.653

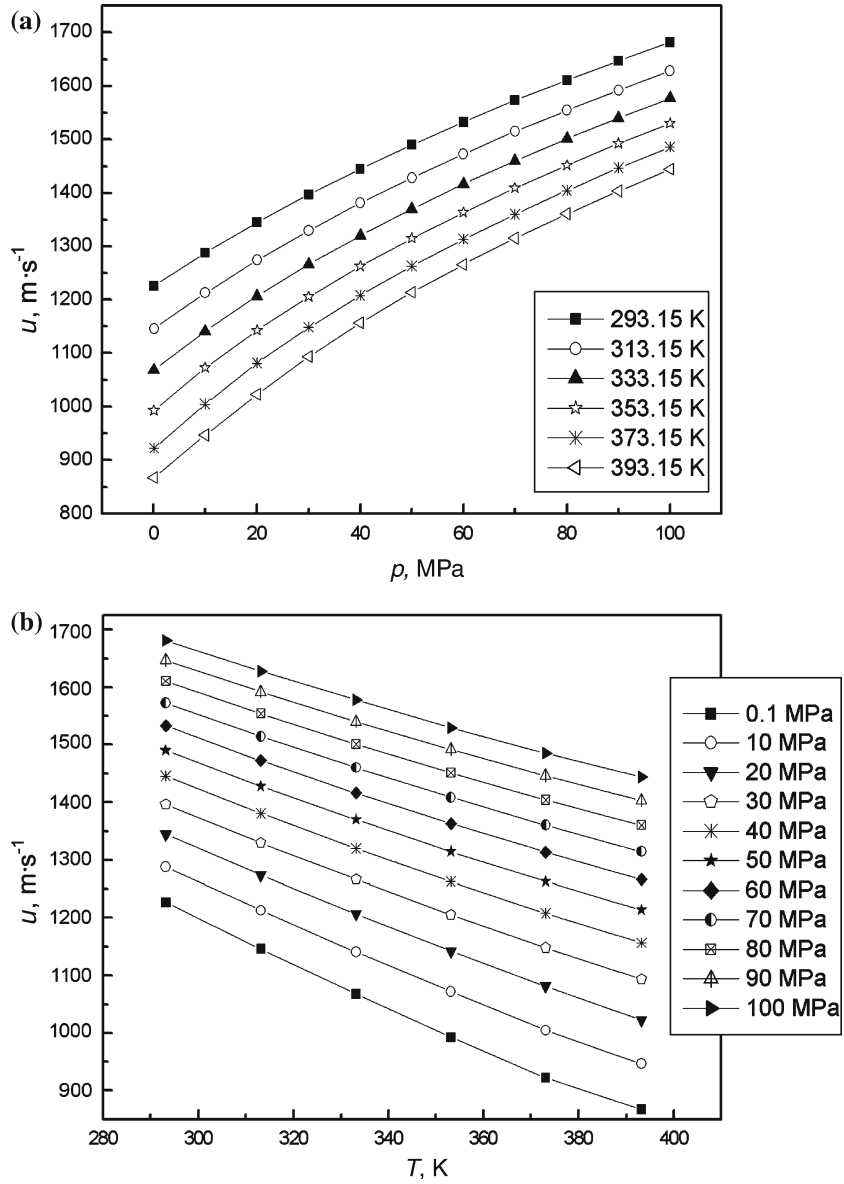

Fig. 2. Speed of sound of nonane: (a) as a function of pressure and (b) as a function of temperature.

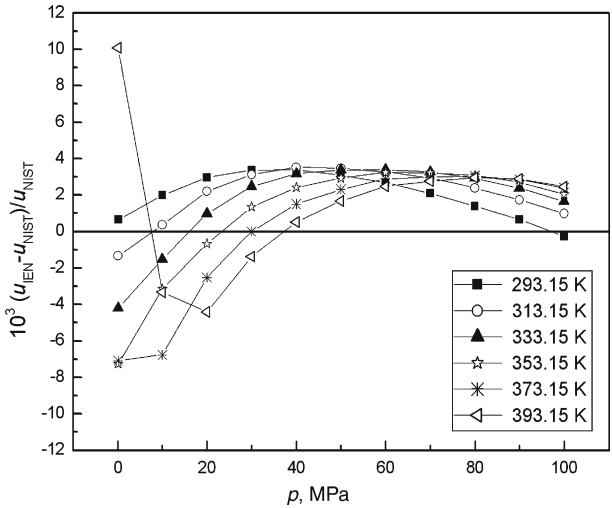

Fig. 3. Deviations of the experimental speed of sound of *n*-nonane from predictions of a dedicated equation of state [4].

atures considered. Because of the low signal-to-noise ratio of each sampled echo at 393.15 K and 0.1 MPa, the corresponding speed-of-sound value should be rejected as a consequence of a less accurate determination of the difference between the two fly times. In this case the deviations from [4] would be less than 0.8%.

Finally our experimental data compare very well with other literature data in overlapping regions: in Fig. 4, comparisons with Boelhouwer [2] and Kling et al. [3] for each isotherm are presented.

3.2. Estimation of the Measurement Uncertainty

The pulse-echo technique for sound-speed determination is an indirect measurement method described by the following model:

$$u_{\text{meas}} = u\,(\Delta L_0, \tau, T, p; \alpha, \beta)\,, \tag{14}$$

where ΔL and τ are independent mechanical determinations, p, T are state variables, and α, β have to be considered as influence quantities [11]. The temperature and pressure are simply parameters of the function u. The speed of sound is determined from mechanical measurements, but gives information on the thermodynamic properties of the fluid. Applying the procedure for the uncertainty propagation to Eq. (14), we obtain,

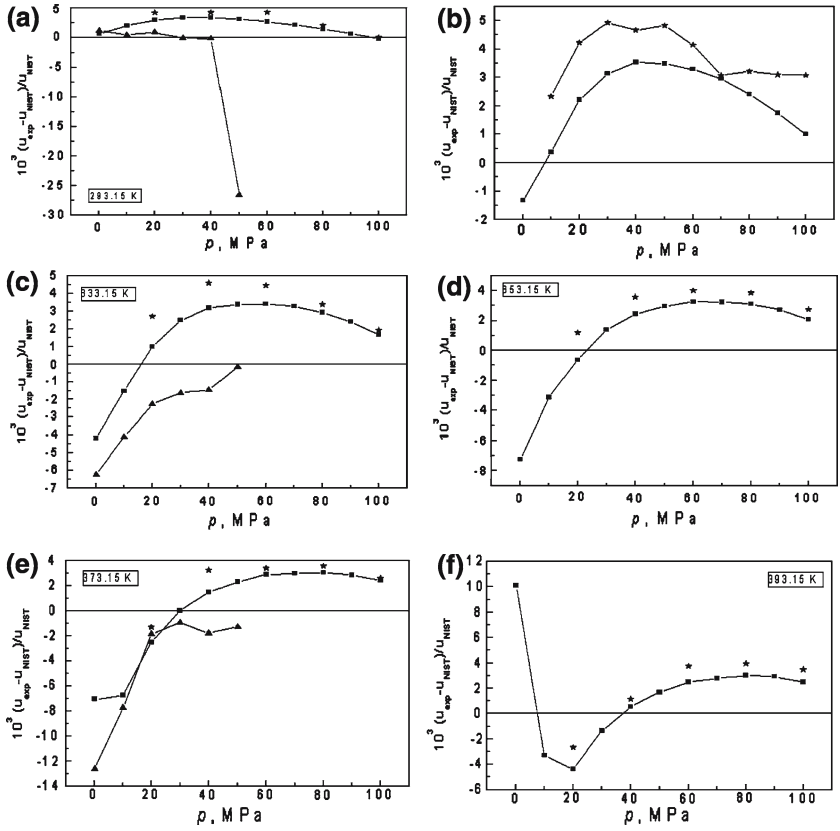

Fig. 4. Deviations of speed-of-sound data of *n*-nonane from equation of state [4]. (a) $T = 293.15$ K: This study, ■; Boelhouwer [2], ★; Kling et al. [3], ▲ (b) $T = 313.15$ K: This study, ■; Boelhouwer [2], ★ (c) $T = 333.15$ K: This study, ■; Boelhouwer [2], ★; Kling et al. [3], ▲ (d) $T = 353.15$ K: This study, ■; Boelhouwer [2], ★ (e) $T = 373.15$ K: This study, ■; Boelhouwer [2], ★; Kling et al. [3], ▲ (f) $T = 393.15$ K: This study, ■; Boelhouwer [2], ★.

as major components of the standard uncertainty, the values listed in Table III.

The uncertainty associated with time-delay measurements is assumed to be equal to 0.5 ns, corresponding to two oscilloscope sampling intervals. Temperature measurements are assumed to be affected by an uncertainty of 0.01 K, corresponding to the calibration accuracy. The uncertainty in the determination of the thermodynamic sound speed depends on an incorrect association of the measured values to the actual thermodynamic $T-p$ state of the sample. The uncertainty of the pressure transducers is

Table III. Uncertainty Budget

Uncertainty source		Relative magnitude
Determination of the acoustic path	$\sigma(\Delta L)/\Delta L$	0.030%
Determination of temporal delay	$\sigma(\tau)/\tau$	0.002%
Temperature measurements	$\left(\frac{\partial u}{\partial T}\right)\frac{\sigma(T)}{u}$	0.004%
Pressure measurements	$\left(\frac{\partial u}{\partial p}\right)\frac{\sigma(p)}{u}$	0.185%
Estimated overall uncertainty		0.19%

better than ± 0.005 MPa for pressures up to 10 MPa and ± 0.2 MPa for higher values; we considered the worst case in the calculation of the uncertainty. The overall relative uncertainty in the sound speed values is estimated to be less than 0.2% over the entire T–p region examined.

The experimental results for the speed of sound compared to the predictions of a dedicated equation of state [4], together with the detailed uncertainty evaluation, have demonstrated the satisfactory performance of the measurement system.

4. CONCLUSIONS

Although *n*-alkanes play a fundamental role in different chemical engineering applications, their thermodynamical properties, in conditions of high temperature and pressure, are not well-known, especially for the chains formed by an odd number of carbon atoms. This work should be considered as the preliminary part of a more in-depth study of this kind of substance, either as pure fluids or as binary and ternary mixtures.

Speed-of-sound measurements on a sample of pure *n*-nonane at high temperature (293.15–393.15 K) and at pressures from 0.1 up to 100 MPa have been discussed and compared with available literature data [2, 3] and the equation of state of [4].

Some possible further improvement can be suggested, namely, a better accuracy in the determination of the acoustic path and an improved piezo-clamping mechanism to guarantee a higher degree of parallelism between the ultrasonic source and reflectors.

REFERENCES

1. S. Lorefice and A. Malengo, *Proc. IV Congress of* "*Metrologia & Qualità*," Turin (2005), pp. 58–62.
2. J. W. M. Boelhouwer, *Physica* **34**:484 (1967).

3. R. Kling, E. Nicolini, and J. Tissot, *Communication au VIII Congrès International de Mécanique Théorique at Appliquée* (1952).
4. E. W. Lemmon and R. Span, *J. Chem. Eng. Data* **51**:785 (2006).
5. G. Benedetto, R. M. Gavioso, P. A. Giuliano Albo, S. Lago, D. Madonna Ripa, and R. Spagnolo, *Int. J. Thermophys.* **26**:1667 (2005).
6. P. J. Kortbeek, M. J. P. Muringer, N. J. Trappeniers, and S. N. Biswas, *Rev. Sci. Instrum.* **56**:1269 (1985).
7. S. J. Ball and J. P. M. Trusler, *Int. J. Thermophys.* **22**:427 (2001).
8. R. Bass, *J. Acoust. Soc. Am.* **30**:602 (1958).
9. ASM Committee on Wrought Stainless Steels, in *Metals Handbook*, 9th Ed. (American Society for Metals, Materials Park, Ohio, 1980).
10. D. Madonna Ripa, R. Gavioso, R. Spagnolo, A. Brighenti, A. Pavan, L. Manara, and M. Schirru, "Misura della velocità del suono in idrocarburi pesanti da Visbreaking (Visbreaking TAR) e analisi delle pulsazioni indotte da un sistema di pompaggio," *Proc. 32nd Convegno Nazionale dell'Associazione italiana di Acustica*, Ancona (2005).
11. R. Vedam and G. Holton, *J. Acoust. Soc. Am.* **43**:108 (1968).